Available online at www.sciencedirect.com
ScienceDirect
Journal of Colloid and Interface Science 303 (2006) 149–158
JOURNAL OF Colloid and Interface Science
www.elsevier.com/locate/jcis

A method to determine the fractal dimension of diesel soot agglomerates

Magín Lapuerta [a,*], Rosario Ballesteros [a], Francisco J. Martos [b]

[a] *Escuela Técnica Superior de Ingenieros Industriales, University of Castilla - La Mancha, Edificio Politécnico, Avda. Camilo José Cela s/n, 13071 Ciudad Real, Spain*

[b] *Departamento de Máquinas y Motores Térmicos, University of Málaga, Plaza del Ejido s/n, 29013 Málaga, Spain*

Received 8 May 2006; accepted 14 July 2006

Available online 28 July 2006

Abstract

Soot agglomerates emitted by diesel engines are composed of primary particle forming irregular clusters. Such irregularity can be quantified by the fractal dimension, whose determination depends on certain parameters not unanimously established, such as the prefactor of the power law relationship. Mean values of the fractal dimension of large collections of agglomerates are usually determined in literature by least-square regression fittings to the power law relationship. In this paper, an iterative method to determine the fractal dimension of individual agglomerates is proposed instead, thus making possible a better discrimination of effects. Functions depending on the fractal dimension and the number of primary particles are proposed for the prefactor and for the overlapping parameter (a measure of the overlap that the primary particles provoke among themselves when projected). Therefore, extreme cases (agglomerates forming a compact sphere and an aligned chain of primary particles) were taken as boundary conditions, for which a geometrical analysis has been performed. The method has been adjusted by comparison with cluster–cluster aggregation models taken from literature, and has proved to have good sensitivity and low loss of information. Some examples are shown from transmission electron microscopy (TEM) images of agglomerates obtained with thermophoretic sampling from the exhaust gas of a diesel engine under different operating conditions.

Keywords: Diesel engines; Fractal dimension; Microscopy; Soot agglomerates

1. Introduction

Diesel soot agglomerates are composed of primary particles with geometries very similar to spheres, as is noted in Fig. 1. Although the mean diameter of the primary particles as well as its standard deviation both have small variations within the engine operating conditions [1,2], it is usual to describe the primary particles as uniform in size (monodisperse) with diameters around 25 nm [3,4]. The primary particles are disposed in the agglomerate as irregular clusters, with different size and compactness, and thus with different apparent densities [5]. Contrary to the primary particles, the agglomerates are not at all uniform in shape nor in size (they are polydisperse), and their description requires statistical approaches.

It is well known that the irregularity of soot particles affects their environmental impact for several reasons: as particles become more irregular their surface increase (and so the adsorption of hydrocarbons), their light extinction efficiency increases (and thus their opacity and global warming or dimming potential, depending on the land surface brightness), their aerodynamic behavior changes (reducing their velocity in ground deposition and increasing the probability of human breathing), their filtering efficiency increases, etc. [6]. Other effects of the irregularity of particles are related to their transport properties (affecting mass, energy and momentum diffusion), their heat radiation properties, etc. [7]. The most common way to quantify this irregularity is by using the fractal dimension, as explained by Mandelbrot [8]. References [1,9–11] are just a few interesting examples of soot applications.

As the distance from the agglomerate's center of gravity increases, the probability of soot primary particles occupying a given space decreases. This probability can be statistically described with an autocorrelation function [9]. In the event that

* Corresponding author. Fax: +34 926295361.
E-mail address: magin.lapuerta@uclm.es (M. Lapuerta).

0021-9797/$ – see front matter
doi:10.1016/j.jcis.2006.07.066

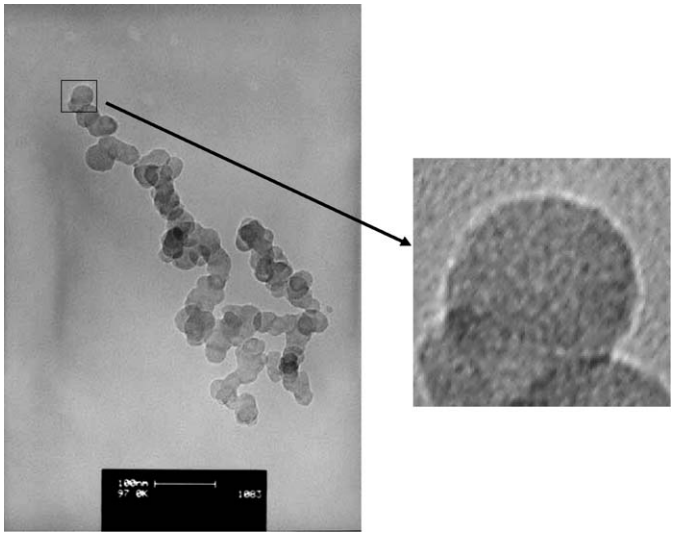

Fig. 1. Diesel soot agglomerate composed of spherical primary particles.

the agglomerate possesses scale similarity, the decrease of the autocorrelation function can be quantified through a negative exponent affecting the distance from the center [12,13]. The fractal dimension is a number which is linearly opposite to such an exponent: the quicker the rate of decrease of the autocorrelation function mentioned, the higher the fractal dimension. Apart from the intrinsic interest of knowing the fractal dimension of an agglomerate, an integration of the autocorrelation function extended to the whole space surrounding the particle center allows for the estimation of the number of primary particles, n_{po}, composing the agglomerate. This estimation is expressed through the power law relationship for large aggregates [9,14]. The applicability of the power law relationship to smaller aggregates ($n_{po} < 200$), such as diesel soot particles usually are, was shown by Megaridis and Dobbins [15] and has been used by many authors for soot characterization [2,12,16–19],

$$n_{po} = k_f \left(\frac{d_g}{d_{po}} \right)^{D_f}, \tag{1}$$

where k_f is a dimensionless prefactor. Different values are used in literature for this prefactor depending on the nature of the agglomerates, the number of primary particles, and on the definition of the characteristic diameter of the agglomerate, and it has also been shown that it is related to the packing fraction of the agglomerate [20]. The diameter of gyration, d_g, defined as twice the radius of gyration, has been used in Eq. (1). The radius of gyration is also used by many authors dealing with soot images [2,17,21]. The radius of gyration is the distance from the center of gravity of the agglomerate to a point where the entire mass of the agglomerate has to be concentrated for its moment of inertia to be the same as that of the agglomerate.

Mean values of the fractal dimension of large collections of agglomerates are usually determined in literature by least-square regression fittings to the power law relationship. In this paper, an iterative method to determine the fractal dimension of individual agglomerates is proposed instead, thus making possible a better discrimination of effects, such as those of the engine operating conditions.

2. Hypothesis of the method

The following hypotheses are assumed in the method proposed:

- Primary particles are considered to be spherical [22], and thus no sintering or flattening effects are taken into account. Oh and Sorensen [23] showed that, although the effect of sintering is very relevant over the prefactor, it is very small over the fractal dimension finally obtained. Additionally primary particles are considered to be homogeneous in size, based on the works by Mathis et al. [24], who showed that variations in the diameter are small when the engine operating conditions are modified, and by Bushell and Amal [25], who showed that the fractal structure is unaffected by the primary particle size distribution. A value of 25 nm was taken for the primary diameter, this being very close to the average diameter of all the measured primary particles.
- Primary particles are considered to be homogeneous in density, based on the uniformity of the interlayer spacing of graphite structures [26], and on the works by Braun et al. [27] who showed that the diesel soot interlayer spacing is very similar to that of graphite structures, and by Vander Val et al. [28], who showed that different thermal exposures modify the number of staked layers, their alignment and their length, but not their interlayer distances. A value of soot density of 1850 kg/m^3 was taken, this being determined from the carbonous layer spacing model proposed by Belenkov [26].
- No preferential orientations are considered in the projected images of the agglomerates, based on the work by Rosner et al. [29], who showed that preferential orientations are nearly canceled by the opposition of thermal forces to incremental drag during thermophoresis sampling. This hypothesis permits a statistically isotropic treatment of nonsymmetric agglomerates, such as those with low fractal dimension.
- The difference between the radius of gyration of the projections and that of the three-dimensional agglomerates is neglected. The former is considered in this work, despite its proven underestimation with respect to the latter [23]. Although the methods based on particle projected images can underestimate the fractal dimension of three-dimensional structures [30], the errors obtained are not very significant [31].
- The moment of inertia of the mass enclosed in the image pixels is neglected, as in other works [32]. This hypothesis has been shown to provide errors on the radius of gyration below 1% when the pixel size remains below 1.3 nm, while the image resolution of all the images processed here leads to a pixel size of 0.43 nm.

As a consequence of the previous hypotheses, the moment of inertia of the agglomerate can be determined as the sum of that of each single primary particle, being the Steiner theorem

applied for each one,

$$I_p = \sum_{i=1}^{n_{po}} m_{po}\left(\frac{3}{5}r_{po}^2 + r_i^2\right) = m_{po}\left(\frac{3}{5}n_{po}r_{po}^2 + \sum_{i=1}^{n_{po}} r_i^2\right), \quad (2)$$

where r_i is the distance from the center of each primary particle to the center of gravity of the agglomerate. The assumption of uniform density for the primary particles allows for the extension of mass conservation to volume conservation [33]:

$$n_{po} = \frac{m_p}{m_{po}} = \frac{V_p}{V_{po}}. \quad (3)$$

Thus, the diameter of gyration is

$$d_g = 2\sqrt{\frac{I_p}{m_p}} = 2\sqrt{\frac{I_p}{n_{po}m_{po}}} = 2\sqrt{\frac{3}{5}r_{po}^2 + \frac{\sum_{i=1}^{n_{po}} r_i^2}{n_{po}}}. \quad (4)$$

This diameter can be determined from the treatment of planar images of the sampled agglomerates, despite the fact that not every primary particle can be accounted for. In practice, a digital analysis of the images allows for the extension of the sum of distances from the center of gravity to every single pixel occupied with particles [32], as a consequence of the last mentioned hypothesis:

$$d_g = 2\sqrt{\frac{\sum_{i=1}^{n_{\text{pixel}}} r_i^2}{n_{\text{pixel}}}}. \quad (5)$$

3. The prefactor of the power law relationship

A literature review presented by Wu and Friedlander [34] shows that authors take values for the prefactor of the power law relationship ranging from 1.05 to 1.59 when the diameter of gyration is used as the characteristic diameter in Eq. (1). However, more recent experimental studies find values for the prefactor of up to 1.9 [35], to 2.74 [33], or even to 8.5 [36]. In general, those values are obtained either from experimental fittings of Eq. (1) or from different models. Recent Monte Carlo simulations for diffusion-limited aggregation regimes lead to propose values for the prefactor around 1.2 [37]. Most of the proposals are constant values, although some authors propose some variation with the void fraction of the agglomerate [34], or with the sintering between primary particles [23]. The last authors, for example, obtained from their modeling an increase of the prefactor with the sintering between primary particles, reaching values of up to $k_f = 3.0$. Other authors [20] showed that the prefactor can be interpreted as a packing coefficient, and calculated it as a function of the fractal dimension and the type of packing. Finally, an expression for the prefactor (denoted as structural coefficient) as a function of the fractal dimension was obtained by Gmachowsky [38] from his aggregation model, reaching values of up to 2.15. In the present work, a function of the fractal dimension and the number of primary particles is proposed for the prefactor. The extreme values for such function correspond to highest fractal dimension and highest packing fraction and to lowest fractal dimension and lowest packing fraction, and have been determined in coherence with the use of the radius of gyration:

- An extreme value of $D_f = 3$ can only be reached in two cases: when the agglomerate is composed of a single primary particle, and when it is composed of a large number of primary particles forming a sphere as compact as possible. In the first case ($n_{po} = 1$), substituting the diameter of gyration obtained from Eq. (4) in Eq. (1),

$$k_f(D_f = 3; n_{po} = 1) = \left(\frac{5}{3}\right)^{3/2} = 2.1517, \quad (6)$$

which is in agreement with that obtained from the model proposed by Gmachowsky [38] for $D_f = 3$. However, this case does not correspond to a fractal structure. In the second case, if the number of composing primary particles is large enough ($n_{po} \to \infty$), the spherical agglomerate can be considered to be homogeneous, and the diameter of gyration is that of a sphere comprising all the primary particles. The maximum packing fraction corresponds to the hexagonal close pack:

$$p = n_{po}\left(\frac{d_g}{d_{po}}\right)^3 = \frac{\pi}{\sqrt{18}}. \quad (7)$$

Combining the power law relationship with the packing fraction expression (Eqs. (1) and (7)),

$$k_f\left(\frac{d_g}{d_{po}}\right)^3 = n_{po} = p\left(\frac{d_p}{d_{po}}\right)^3 \to k_f(D_f = 3; n_{po} \to \infty) = \frac{\pi}{\sqrt{18}}\left(\frac{d_p}{d_g}\right)^3. \quad (8)$$

As Eq. (4) is again applicable in this case, the prefactor takes a value, independently of the number of primary particles, of

$$k_f(D_f = 3) = \frac{\pi}{\sqrt{18}}\left(\frac{5}{3}\right)^{3/2} = 1.5933. \quad (9)$$

- If the agglomerate is composed of a large number of aligned primary particles with a contact point (case of $D_f = 1$ and lowest packing) the moment of inertia can be obtained by the integration of the square distances from the center of gravity to the center of every primary particle. As shown in Fig. 2, these distances can be obtained as functions of the numeral of the primary particle:

$$r_i = (n_i - 1)r_{po}. \quad (10)$$

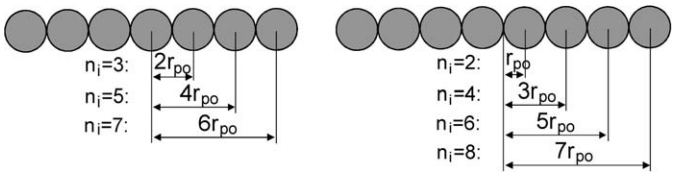

Fig. 2. Distances from the center of gravity to the center of primary particles for odd (left) and even (right) numerals.

The moment of inertia of the agglomerate is

$$I_p = m_{po}\left[\frac{3}{5}n_{po}r_{po}^2 + \int_0^{n_{po}}(n_i-1)^2 r_{po}^2\,\mathrm{d}n_i\right]$$
$$= m_{po}n_{po}r_{po}^2\left(\frac{n_{po}^2}{3} - n_{po} + \frac{8}{5}\right), \tag{11}$$

and thus the characteristic diameter is

$$d_g = 2\sqrt{r_{po}^2\left(\frac{n_{po}^2}{3} - n_{po} + \frac{8}{5}\right)}$$
$$= 2r_{po}n_{po}\sqrt{\frac{1}{3} - \frac{1}{n_{po}} + \frac{8}{5n_{po}^2}}. \tag{12}$$

Substituting this diameter in the power law relationship, Eq. (1), with $D_f = 1$, and solving for k_f,

$$k_f(D_f = 1) = \frac{1}{\sqrt{\frac{1}{3} - \frac{1}{n_{po}} + \frac{8}{5n_{po}^2}}}. \tag{13}$$

If the number of primary particles is very large, the prefactor tends toward

$$k_f(D_f = 1; n_{po} \to \infty) = \sqrt{3} = 1.7321. \tag{14}$$

A potential function is proposed for this prefactor (when the number of primary particles is very large) in order to connect the extreme values obtained within the range $D_f \in [1\text{–}3]$ and to provide a smooth approximation to the values corresponding to $D_f = 1$, as the void fraction of a chain-like structure tends toward that of an aligned chain of particles. In addition, the shape of this function can be modulated with the shape parameter m, as shown in Fig. 3 (for $n_{po} = \infty$), for values of m ranging from 1.5 to 3. This modulation permits, as shown below, an adjustment to experimental or modeled results from literature in the diffusion limited or ballistic aggregation regimes:

$$k_f(n_{po} = \infty) = 0.7321 + 0.8612^{(\frac{D_f-1}{2})^m}. \tag{15}$$

If the number of primary particles is not very large, as is usually the case of diesel soot agglomerates, a better estimate of the prefactor is given by the following generic potential function, which encloses expression (13). The effect of the number of primary particles on this function can be observed in Fig. 4:

$$k_f = k_f(D_f = 1) - 1$$
$$+ \left(1 + k_f(D_f = 3) - k_f(D_f = 1)\right)^{(\frac{D_f-1}{2})^m}. \tag{16}$$

This general expression for the prefactor provides values always higher than 1.5933, depending on the fractal dimension of the agglomerate and on the number of primary particles. Many of the above mentioned values of k_f proposed in literature are, in general, close to those proposed here, but none considers the combined effect of the fractal dimension and the number of primary particles. Disagreements with some of the most reliable values proposed in literature could be, however, caused by some of the hypotheses described in Section 2, such as the obtention

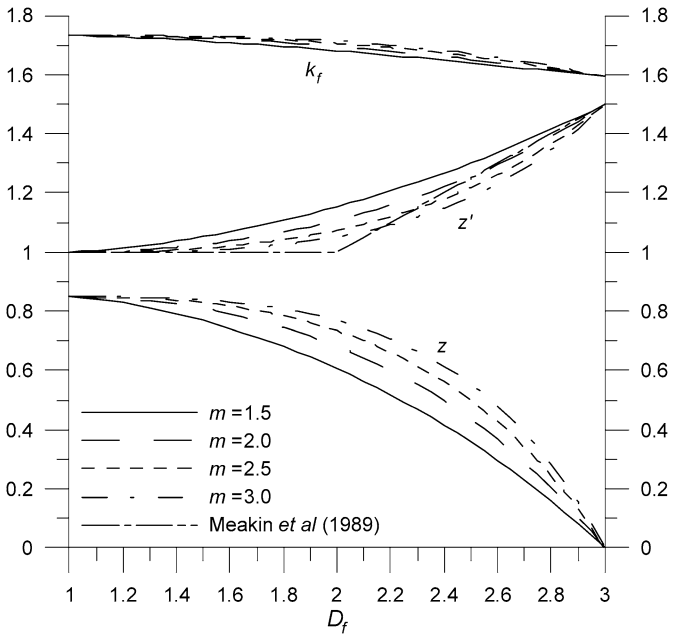

Fig. 3. Prefactor of the power law relationship, overlapping factor and overlapping coefficient vs fractal dimension for large agglomerates and for different values of the shape parameter.

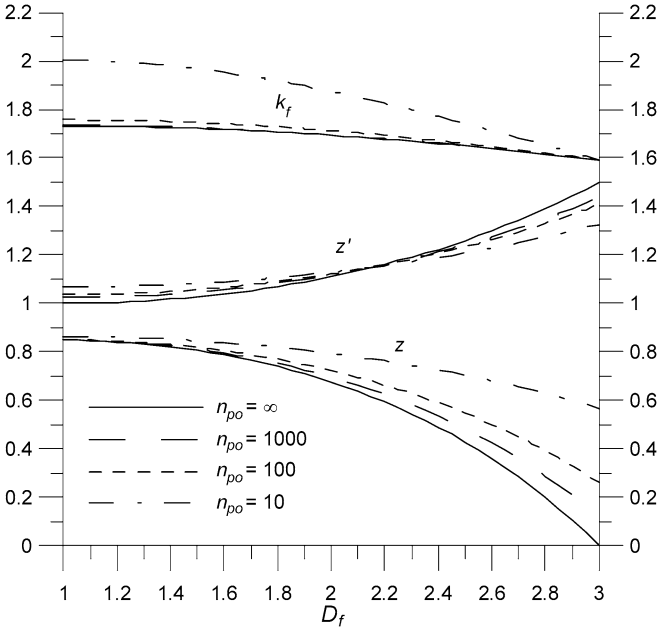

Fig. 4. Prefactor of the power law relationship, overlapping factor and overlapping coefficient vs fractal dimension for different number of primary particles and for a shape parameter $m = 1.95$.

of the radius of gyration from projected images, or by the association of the maximum packing fraction with the maximum fractal dimension (Section 3).

Determining the power law prefactor alone is not enough to calculate the fractal dimension of the agglomerate, because the number of primary particles is unknown. The visible number of primary particles is certainly lower than that obtained from a spatial integration of the autocorrelation function along the radial distance from the particle center. In consequence, further

analysis of the visibility of primary particles in the images must be made.

4. The overlapping factor and the overlapping exponent

In contrast to the conservation of primary particles mass and volume, no conservation can be accepted for the projected surface of primary particles [30], unless an overlapping coefficient, z, is included. A linear overlapping factor is defined here as the ratio between the projected area of the agglomerate and the area which the whole number of primary particles composing the agglomerate would project isolately:

$$A_p = z n_{po} A_{po}. \tag{17}$$

This definition of the linear overlapping factor is different to those proposed by other authors [23,39]. Combining Eqs. (3) and (17) leads to the following expression for the overlapping factor:

$$z = \frac{V_{po}}{V_p}\frac{A_p}{A_{po}}. \tag{18}$$

If primary particles are assumed to be spherical, this expression turns into

$$z = \frac{2d_{po}}{3}\frac{A_p}{V_p}. \tag{19}$$

The volume of the agglomerate cannot be measured by any optical method, but it can be calculated from an estimated overlapping factor. The overlapping factor decreases as the fractal dimension of the agglomerate increases. In order to quantify this factor, the following extreme cases have been analyzed:

- If the agglomerate is composed of a large number of primary particles forming a sphere, the overlapping factor can be directly obtained from Eq. (19), or even expressed as a function of the number of primary particles, using Eq. (3),

$$z(D_f = 3) = \frac{2d_{po}}{3}\frac{3}{2d_p} = \frac{d_{po}}{d_p} = \frac{1}{n_{po}^{1/3}}, \tag{20}$$

  which tends toward zero when the number of particles is very large:

$$z(D_f = 3; n_{po} = \infty) = 0. \tag{21}$$

- If the agglomerate is composed by two primary particles with a contact point (Fig. 5, left), then the overlapping factor depends on the angle between the axis (line connecting the centers of the particles) and the projection plane. The hidden projected area is

$$A_h = r_{po}^2(2\varphi - \sin 2\varphi). \tag{22}$$

  The overlapping factor is then

$$z(\varphi) = 1 - \frac{A_h}{n_{po}A_{po}} = 1 - \frac{A_h}{2A_{po}} = 1 - \frac{2\varphi - \sin 2\varphi}{2\pi}. \tag{23}$$

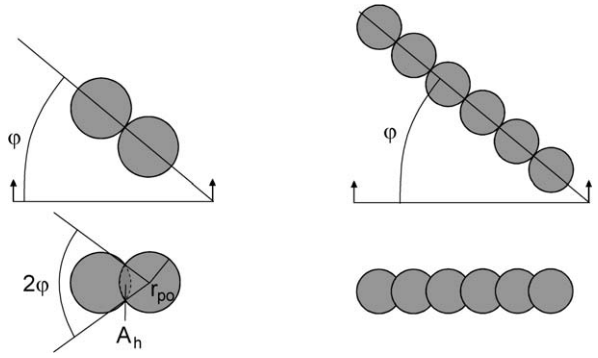

Fig. 5. Overlap between two contacting spheres (left) and between a large number of aligned spheres (right).

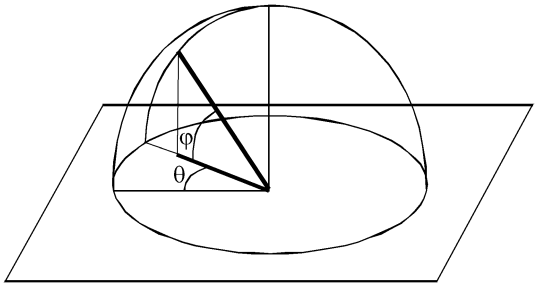

Fig. 6. Hemispheric averaging of the overlapping factor in the projection of linear agglomerates.

- If the agglomerate is composed of a large number of aligned primary particles with a contact point (Fig. 5, right), then the overlapping factor also depends on the angle between the axis and the projection plane. The hidden projected area is now

$$A_h = (n_{po} - 1)r_{po}^2(2\varphi - \sin 2\varphi). \tag{24}$$

  The overlapping factor is then

$$z(\varphi) = 1 - \frac{A_h}{n_{po}A_{po}} = 1 - \frac{(n_{po} - 1)(2\varphi - \sin 2\varphi)}{n_{po}\pi}. \tag{25}$$

  As the angle between linear agglomerate and the projection plane is arbitrary, the overlapping factor can be calculated as an average of the individual factors corresponding to all possible orientations. For such averaging, integration in spherical coordinates was made along the visible hemisphere (Fig. 6):

$$z(D_f = 1) = \frac{\int_0^{2\pi}\int_0^{\frac{\pi}{2}} z(\varphi)\cos\varphi\,\mathrm{d}\varphi\,\mathrm{d}\theta}{\int_0^{2\pi}\int_0^{\frac{\pi}{2}} \cos\varphi\,\mathrm{d}\varphi\,\mathrm{d}\theta}$$

$$= \frac{2\pi\left[\int_0^{\frac{\pi}{2}} \cos\varphi\,\mathrm{d}\varphi - \frac{2(n_{po}-1)}{\pi n_{po}}\int_0^{\frac{\pi}{2}} \varphi\cos\varphi\,\mathrm{d}\varphi + \frac{(n_{po}-1)}{\pi n_{po}}\int_0^{\frac{\pi}{2}} \sin 2\varphi\cos\varphi\,\mathrm{d}\varphi\right]}{2\pi}$$

$$= \frac{8}{3\pi} + \frac{1}{n_{po}}\left(1 - \frac{8}{3\pi}\right) = 0.8488 + \frac{0.1512}{n_{po}}. \tag{26}$$

  When the number of primary particles is very large, this expression turns into

$$z(D_f = 1; n_{po} = \infty) = 0.8488. \tag{27}$$

Consequently, an expression for the overlapping factor should provide variations within the domain [0–0.8488] depending on the fractal dimension and the number of primary particles of the agglomerate.

However, most authors [1,15] consider the overlapping effect by means of another type of expression, as firstly proposed by Medalia and Heckman [40]:

$$n_{po} = \left(\frac{A_p}{A_{po}}\right)^{z'}. \tag{28}$$

As z' also expresses the overlapping through a potential expression, it is denoted here as an overlapping exponent. Different values for the overlapping exponent have been proposed in literature: Medalia and Heckman [40] used $z' = 1.15$, while many others [15,36,41] coincidentally obtained $z' = 1.09$ from different experimental procedures. However, none of these constant-values is consistent with the proved dependence of the overlapping effect with the irregularity of the agglomerate. Other authors considered such dependency: Meakin et al. [7] proposed different fits for this exponent from the results of his model for different aggregation regimes, and finally observed that, in general, for fractal dimensions higher than 2, this exponent should depend on the fractal dimension as $z' = D_f/2$. In the same range of fractal dimension ($D_f > 2$), Oh and Sorensen [23] proposed $z' = D_f/D_f^*$, where D_f^* is the fractal dimension of the projected area. In the present work, the combination of Eqs. (3) and (28) leads to the following expression for the overlapping exponent:

$$z' = \frac{\ln \frac{V_p}{V_{po}}}{\ln \frac{A_p}{A_{po}}}. \tag{29}$$

The same particular cases are again applied to the last expression:

- If the agglomerate is composed of a large number of primary particles forming a compact sphere, the overlapping exponent can be directly obtained from Eq. (29):

$$z'(D_f = 3) = \frac{3}{2}. \tag{30}$$

- If the agglomerate is composed of a large number of aligned primary particles with a contact point, the overlapping exponent can be obtained by introducing the corresponding overlapping factor (Eq. (26)) in Eq. (29):

$$z'(D_f = 1) = \frac{\ln n_{po}}{\ln\left[n_{po}\left(0.8488 + \frac{0.1512}{n_{po}}\right)\right]} = \frac{\ln n_{po}}{\ln(0.8488 n_{po} + 0.1512)}. \tag{31}$$

When the number of primary particles is very large, this expression tends toward unity:

$$z'(D_f = 1; n_{po} = \infty) = 1. \tag{32}$$

Potential expressions for both the overlapping factor and the overlapping exponent are proposed (in the case of very large agglomerates) in order to simulate a smooth approximation to the values corresponding to $D_f = 1$, in coherence with the proposed function for the prefactor of the power law relationship, and because the overlap between particles belonging to chain-like structures tends toward that of an aligned chain of particles:

$$z(n_{po} = \infty) = 1.8488 - 1.8488^{\left(\frac{D_f - 1}{2}\right)^m}, \tag{33}$$

$$z'(n_{po} = \infty) = 1.5^{\left(\frac{D_f - 1}{2}\right)^m}. \tag{34}$$

The shape of these equations can be modulated by means of the shape parameter m, as shown in Fig. 3 for values of m ranging from 1.5 to 3. The shape of the overlapping exponent proposed by Meakin et al. [7] is also shown in the figure for comparison.

If the number of primary particles is not very large, a better estimate of the overlapping effect is given by the following generic potential functions, which enclose expressions (20), (26) and (31). The effect of the number of primary particles on these functions is observed in Fig. 4:

$$z = z(D_f = 1) + 1 - \left(z(D_f = 1) + 1 - z(D_f = 3)\right)^{\left(\frac{D_f - 1}{2}\right)^m}, \tag{35}$$

$$z' = z'(D_f = 1) - 1 + \left(2.5 - z'(D_f = 1)\right)^{\left(\frac{D_f - 1}{2}\right)^m}. \tag{36}$$

These general expressions for the overlapping factor and the overlapping exponent provide variations within the domains [0–0.8488] and [1–1.5], respectively, depending on the fractal dimension of the agglomerate. In the case of the overlapping exponent, this domain is the same as those proposed by both Meakin et al. [7] and Oh and Sorensen [23].

5. Selection and adjustment of the proposed method

The relationships between the number of primary particles and the overlapping factor (17) or exponent (28), together with the power law (1), to eliminate the unknown number of primary particles, and to finally calculate the fractal dimension. The two resulting equations are

$$k_f \left(\frac{d_g}{d_{po}}\right)^{D_f} = \frac{1}{z}\frac{A_p}{A_{po}}, \tag{37}$$

$$k_f \left(\frac{d_g}{d_{po}}\right)^{D_f} = \left(\frac{A_p}{A_{po}}\right)^{z'}. \tag{38}$$

An iterative process is proposed for solving any of these equations, as shown in Fig. 7.

In order to select the method (linear, Eq. (37), or potential, Eq. (38)) both linear and potential methods were applied with different values of the shape parameter for the determination of the fractal dimension of 1734 images of soot agglomerates. These images were obtained with a high resolution transmission electron microscopy (TEM) Phillips CM-200 microscope, whose point resolution is lower than 2 Å at an accelerating voltage of 200 kV, an then they were processed using an image editing utility to separate the aggregates into their own bitmap

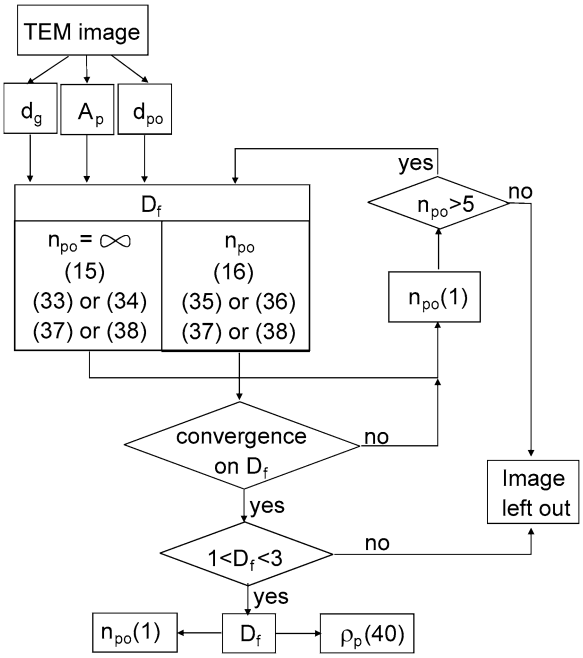

Fig. 7. Scheme of the iterative method. Numbers indicate equations.

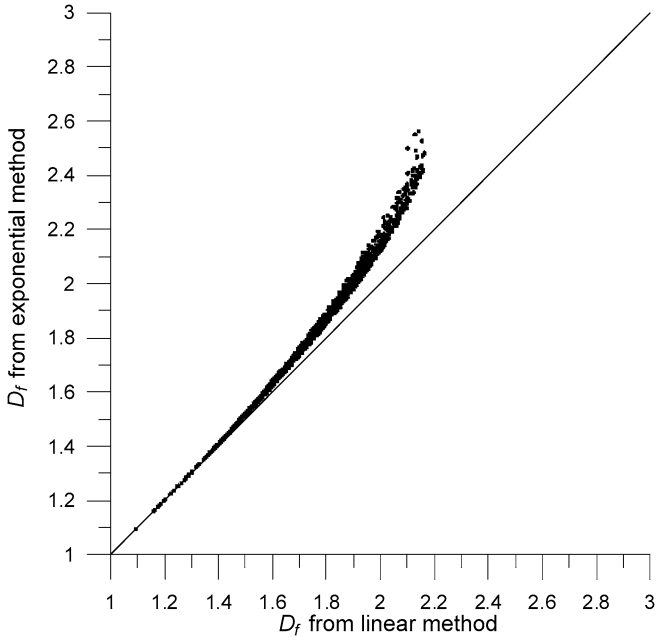

Fig. 8. Fractal dimensions resulting from the potential method vs those from the linear method (with $m = 1.95$).

images and remove any extraneous dark pixel from the background [25]. The samples were obtained with a thermophoretic soot sampling device (TSSD). The TSSD collected soot particles in 3 mm diameter Formvar-coated copper grids (Pelco No. 160), via a hole drilled in a vertical direction through the exhaust pipe of a 2.2 L four-cylinder direct-injection Diesel engine (Nissan YD2.2) with rated power of 84 kW at a speed of 4000 rpm, typical of vehicle transportation in Europe. The collected samples correspond to engine operation modes sweeping wide ranges of engine speed, load and exhaust gas recirculation.

The method expressed by Eq. (38) was preferred to that expressed by Eq. (37), because the values of fractal dimensions spread out along a wider range, for every value of m, as shown in Fig. 8 for $m = 1.95$ as an example. Consequently, the sensitivity of the potential method is higher than that of the linear one. Additionally, the potential method is commonly used in literature.

Once the fractal dimension is obtained, the application of this method makes it possible to calculate the number of primary particles composing the aggregate, with Eq. (1) (see Fig. 7). For the selection of the shape parameter, comparisons were made between the resulting numbers of primary particles (obtained with different values of the shape parameters) and those obtained from the models proposed by Meakin et al. [7] for diffusion-limited aggregation (Fig. 9, left) and for ballistic aggregation without restructuring (Fig. 9, right). This is based on the evidence that when particles are sampled from the exhaust pipe, their structure corresponds to aggregation either under ballistic or under diffusion-limited regimes, depending on the gas temperature, the mean free particle path and the particle size [42], and thus on the engine operating conditions. For the former comparison only images of aggregates whose fractal dimension obtained belonged to a range [1.78–1.82] were taken, this range corresponding to a narrow bracket around the typical fractal dimension proposed by this author in the diffusion-limited aggregation regime: $1.80 \pm 1\%$. For the latter comparison only images of aggregates with a fractal dimension belonging to [1.93–1.97] were taken, which corresponds to a bracket around the typical fractal dimension proposed in the ballistic aggregation regime: $1.95 \pm 1\%$. The fitting of the data to the diffusion-limited aggregation model yielded a shape parameter $m = 1.85$ whereas the fitting to the ballistic aggregation model led to a value of $m = 2.05$. A mean value of such numbers was taken as the shape parameter for the present method, as such regimes are considered to be dominant in the aggregation process of soot particles along the exhaust pipe:

$$m = 1.95. \tag{39}$$

The application of the finally adjusted method (Eqs. (16), (36), (38) and (39)) to the 1734 images resulted in 1454 valid cases, with is a 84% success rate. 128 images were finally left out (see Fig. 7) either because the number of primary particles obtained was lower than 5 (12.5% of the cases) or because no solution within the range $1 < D_f < 3$ was found (3.5% of the cases). This lower limit $n_{po} = 5$ is in agreement with many authors [9,27,36], and is justified because the applicability of the power law relationship becomes inappropriate.

6. Application of the proposed method

Although the application of this method is not the objective of this paper, Figs. 10 and 11 show, as examples, six TEM images together with their resulting fractal dimensions. It can be observed that the proposed method is able to provide a differentiated numerical description of the fractal dimension, and consequently of the irregularity of the agglomerates, within the typical operation range of modern diesel engines. Other interesting results are also derived from the fractal dimension ob-

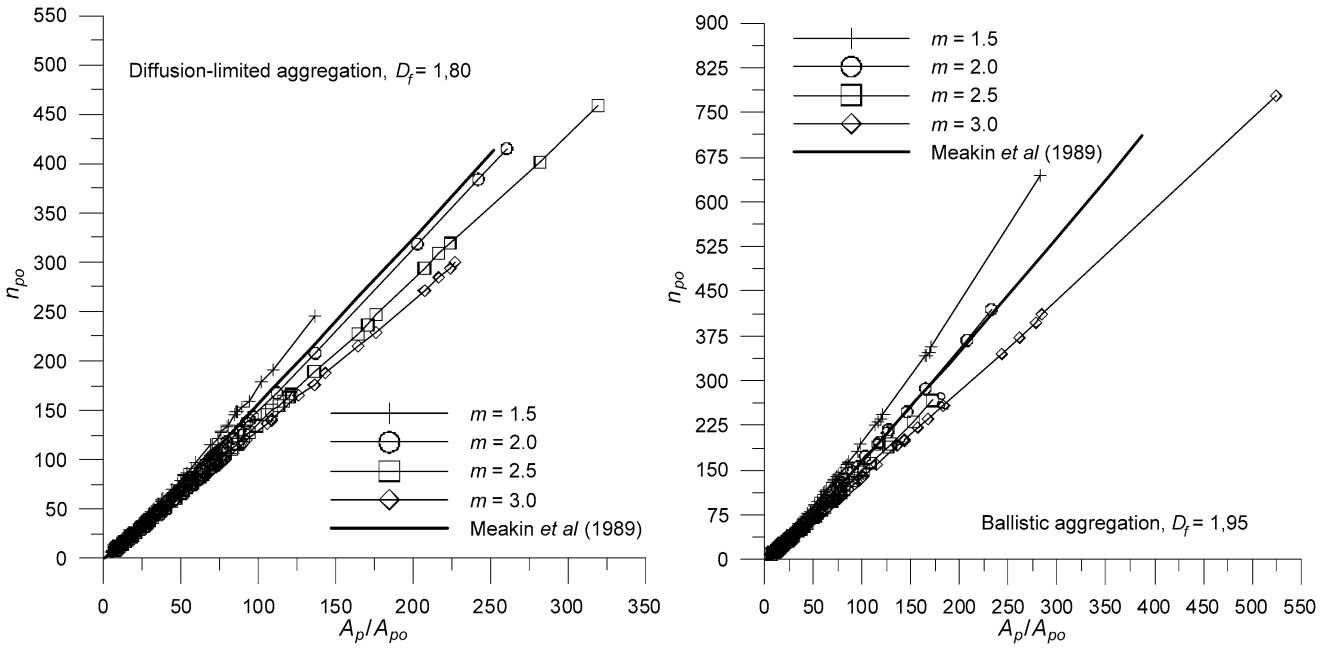

Fig. 9. Comparison of n_{po} results with results from modeling by Meakin et al. [7] for aggregates with characteristic fractal dimensions of the diffusion-limited aggregation regime (left) and of the ballistic aggregation regime (right) for different values of the shape parameter.

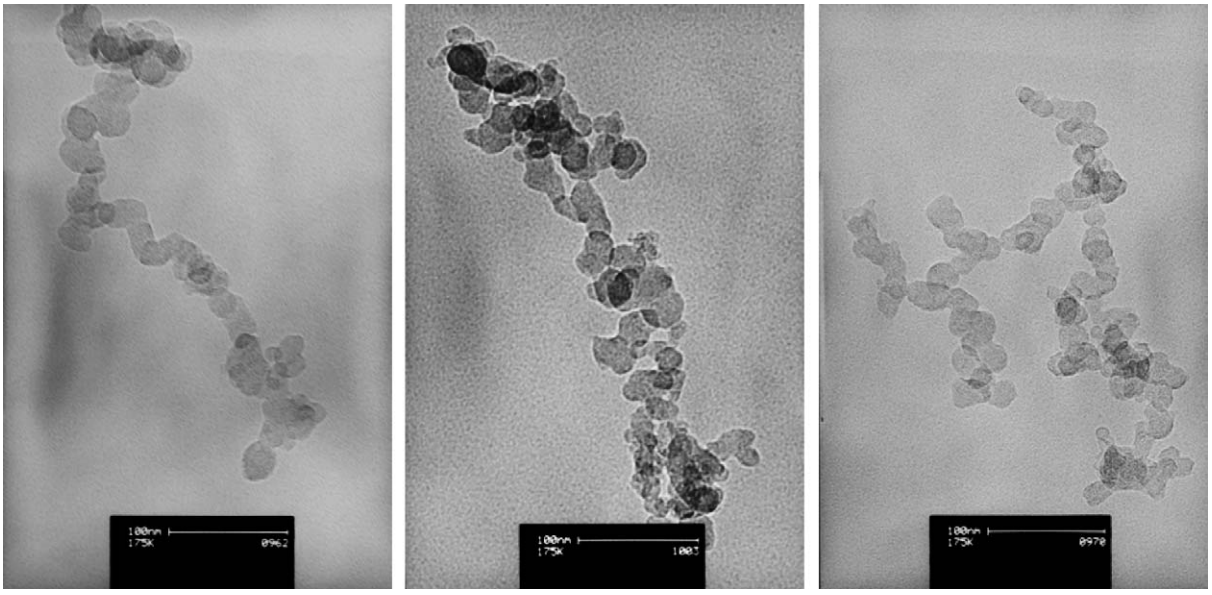

Fig. 10. Soot images taken with TEM with resulting fractal dimensions of 1.42 (left), 1.57 (center) and 1.75 (right) using the proposed method.

tained, such as the number of primary particles, the volume of the agglomerate and its apparent density [34,43]:

$$\rho_p = \frac{n_{po} m_{po}}{V_g} = n_{po} \left(\frac{d_{po}}{d_g} \right)^3 \rho_s = k_f \left(\frac{d_g}{d_{po}} \right)^{D_f - 3} \rho_s. \qquad (40)$$

The application of this method can be illustrated with the abacus shown in Fig. 12, where level curves for fractal dimension, number of primary particles and particle apparent density are shown in different colors. Dots for each of the 1454 valid images of agglomerates have been also included in the figure. This results show a mean fractal dimension of $\overline{D}_f = 1.87$ and a mean number of primary particles of $\overline{n_{po}} = 81.2$, which are quite in agreement with literature on diesel soot.

7. Conclusions

A method to determine the fractal dimension of soot agglomerates, as an indicator of their irregularity, has been developed and fitted to the results of cluster–cluster aggregation models taken from literature. The method is based on the determination of the prefactor of the power law relationship and an overlapping parameter as functions of the fractal dimension and the number of primary particles, by means of potential inter-

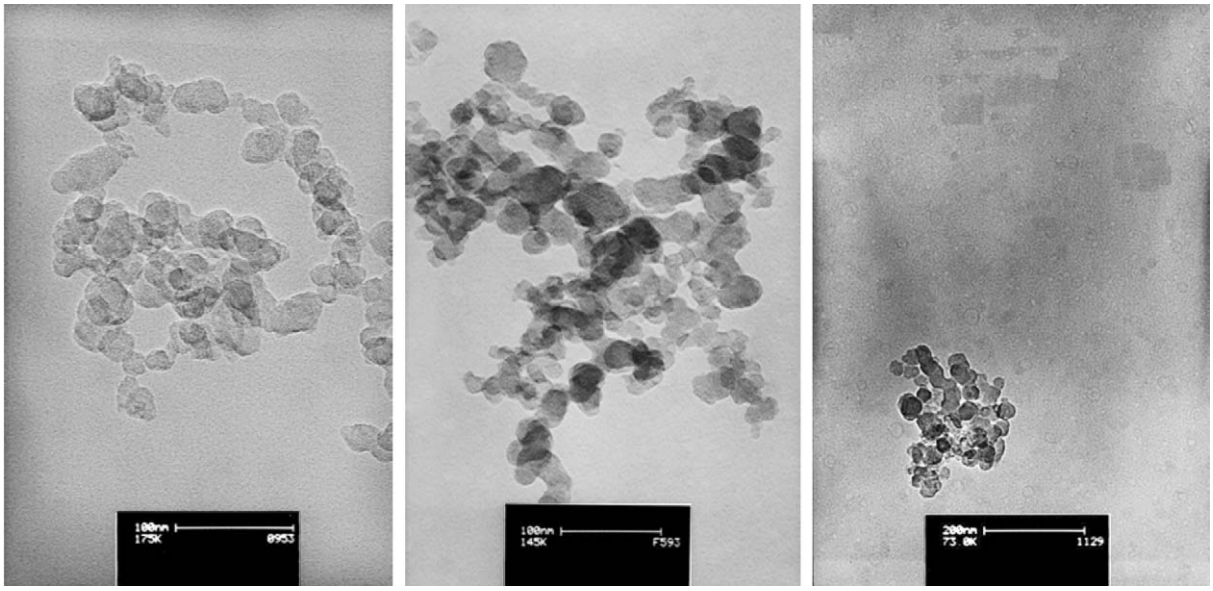

Fig. 11. Soot images taken with TEM with resulting fractal dimensions of 2.10 (left), 2.32 (center) and 2.73 (right) using the proposed method.

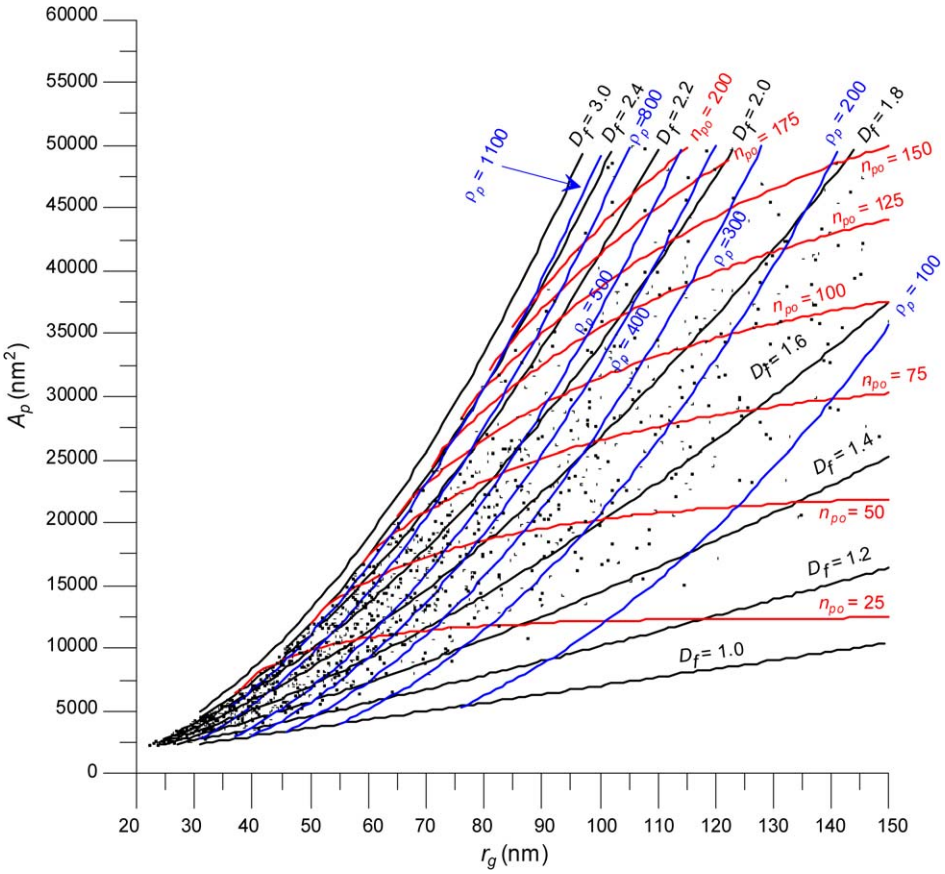

Fig. 12. Abacus for the particle morphological characterization from TEM images.

polations between the extreme cases (agglomerates forming a sphere with highest compactness and an aligned chain of primary particles). A literature review has shown that there is no consensus about the values of these parameters. Although the overlapping parameter does not necessarily have to be an exponent, the overlapping exponent provides better sensitivity. The proposed iterative method has proved useful for the application of TEM images from the thermophoretic sampling of soot particles from the exhaust pipe of a diesel engine, with good sensitivity and a low proportion of left-out images, which is essential for a good discrimination of the effect of the engine operating conditions. An abacus including the results of a col-

lection of 1454 images shows that, although the method was adjusted for a specific aggregation regime, it provides a wide range of results within the fractal dimension limits. These results agree to a large extent with results obtained by different authors either from modeling or from experimental works.

Acknowledgment

The authors wish to acknowledge Ninon Larche for correcting the English.

Appendix A. Nomenclature

A	Projected area
D	Dimension
d	Diameter
I	Moment of inertia
k	Prefactor
m	Shape parameter of mathematical functions
n	Number
r	Radius or distance from the center of gravity
V	Volume
z	Overlapping factor
z'	Overlapping exponent
ρ	Density
φ	Angle between the agglomerate axis and the projection plane
θ	Angle of the projected agglomerate axis

Subscripts

f	fractal
g	gyration
h	hidden
i	numeral of the primary particle in the agglomerate
p	particle or agglomerate
po	primary particle
s	soot

References

[1] K.O. Lee, J. Zhu, S. Ciatti, A. Yozgatligil, M.Y. Choi, SAE paper 2003-01-3169, 2003.
[2] J. Zhu, K.O. Lee, R. Sekar, M.Y. Choi, in: Proceedings of the Third Joint Meeting of the U.S. Sections of the Combustion Institute, 2003.
[3] G.J. Smallwood, D. Clavel, D. Gareau, R.A. Sawchuk, D.R. Snelling P.O. Witze, B. Axelsson, W. Bachalo, Ö.L. Gülder, SAE paper 2002-01-2715, 2002.
[4] M. Wentzel, H. Gorzawski, K.H. Naumann, H. Saathoff, S. Weinbruch, J. Aerosol Sci. 34 (2003) 1347.
[5] M. Lapuerta, O. Armas, A. Gómez, Aerosol Sci. Technol. 37 (2003) 369.
[6] D.B. Kittelson, J. Aerosol Sci. 29 (1998) 575.
[7] P. Meakin, B. Donn, G.W. Mulholland, Langmuir 5 (1989) 510.
[8] B.B. Mandelbrot, The Fractal Geometry of Nature, W.H. Freeman, New York, 1983.
[9] R.J. Samson, G.W. Mulholland, J.W. Gentry, Langmuir 3 (1987) 272.
[10] C. Van Gulijk, J.C.M. Marijnissen, M. Makkee, J.A. Moulijn, A. Schmidt-Ott, J. Aerosol Sci. 35 (2004) 633.
[11] A.V. Filippov, M. Zurita, D.E. Rosner, J. Colloid Interface Sci. 229 (2000) 261.
[12] J. Cai, N. Lu, C.M. Sorensen, J. Colloid Interface Sci. 171 (1995) 470.
[13] S.K. Friedlander, Smoke, Dust and Haze. Fundamentals of Aerosol Dynamics, Oxford Univ. Press, New York, 2000.
[14] R. Botet, R. Jullien, Ann. Phys. 13 (1988) 153.
[15] C.M. Megaridis, R.A. Dobbins, Combust. Sci. Technol. 71 (1990) 95.
[16] B. Gorbunov, A.G. Clarke, R.S. Hamilton, J. Aerosol Sci. 30 (1999) S445.
[17] K.O. Lee, R. Cole, R. Sekar, M.Y. Choi, J. Kang, C. Bae, H. Shin, Proc. Combust. Inst. 29 (2002) 647.
[18] M. Zurita-Gotor, D.E. Rosner, J. Colloid Interface Sci. 255 (2002) 10.
[19] K. Park, D.B. Kittleson, P.H. McMurry, Aerosol Sci. Technol. 38 (2004) 881.
[20] C.M. Sorensen, G.C. Roberts, J. Colloid Interface Sci. 186 (1997) 447.
[21] K.O. Lee, J. Zhu, SAE paper 2004-01-1981, 2004.
[22] K.E.J. Lehtinen, M.R. Zachariah, J. Aerosol Sci. 33 (2002) 357.
[23] C. Oh, C.M. Sorensen, J. Colloid Interface Sci. 193 (1997) 17.
[24] U. Mathis, M. Mohr, R. Kaegi, Environ. Sci. Technol. 39 (2005) 1887.
[25] G. Bushell, R. Amal, J. Colloid Interface Sci. 205 (1998) 459.
[26] E.A. Belenkov, Inorg. Mater. 37 (2001) 1094.
[27] A. Braun, F.E. Huggins, S. Seifert, J. Ilavsky, N. Shah, K.E. Kelly, A. Sarofim, G.P. Huffman, Combust. Flame 137 (2004) 63.
[28] R.L. Vander Val, A.J. Tomasek, K. Street, D.R. Hull, W.K. Thompson, Appl. Spectrosc. 58 (2004) 230.
[29] D.E. Rosner, D.W. Mackowski, P. García-Ybarra, Combust. Sci. Technol. 80 (1991) 87.
[30] S.N. Rogak, R.C. Flagan, Part. Part. Syst. Charact. 9 (1992) 19.
[31] J.A. Nelson, R.J. Crookes, S. Simons, J. Phys. D Appl. Phys. 23 (1990) 465.
[32] C.M. Sorensen, W.B. Hageman, Langmuir 17 (2001) 5431.
[33] Ü.Ö. Köylü, C.S. McEnally, D.E. Rosner, L.D. Pfefferle, Combust. Flame 110 (1997) 494.
[34] M.K. Wu, S.K. Friedlander, J. Colloid Interface Sci. 159 (1993) 246.
[35] A. Neer, Ü.Ö. Köylü, Combust. Flame 146 (2006) 142.
[36] Ü.Ö. Köylü, G.M. Faeth, T.L. Farias, M.G. Carvalho, Combust. Flame 100 (1995) 621.
[37] M. Lattuada, H. Wu, M. Morbidelli, J. Colloid Interface Sci. 268 (2003) 106.
[38] L. Gmachowsky, Colloids Surf. A Physicochem. Eng. Aspects 211 (2002) 197.
[39] A.M. Brasil, T.L. Farias, M.G. Carvalho, J. Aerosol Sci. 30 (1999) 1379.
[40] A.I. Medalia, F.A. Heckman, Carbon 7 (1969) 567.
[41] J. Cai, N. Lu, C.M. Sorensen, Langmuir 9 (1993) 2861.
[42] G. Skillas, S. Künzel, H. Burtscher, U. Baltensperger, K. Siegmann, J. Aerosol Sci. 29 (1998) 411.
[43] M.M. Maricq, N. Xu, J. Aerosol Sci. 34 (2004) 1251.